

**ORIGINAL
RESEARCH**

P.W.A. Willems
P.A. Brouwer
J.J. Barfett
K.G. terBrugge
T. Krings

Detection and Classification of Cranial Dural Arteriovenous Fistulas Using 4D-CT Angiography: Initial Experience

BACKGROUND AND PURPOSE: The criterion standard to diagnose and classify cranial DAVFs is DSA. Since this is invasive, relatively expensive and time-consuming, a noninvasive alternative is of interest. We aimed to evaluate the capabilities and pitfalls of 4D-CTA in a consecutive series of patients who presented with a newly diagnosed cranial DAVF, as demonstrated by conventional DSA.

MATERIALS AND METHODS: Eleven patients were included in this study after biplane DSA demonstrated a cranial DAVF. They subsequently underwent 4D-CTA imaging by using a 320-detector CT scanner. DSA and 4D-CTA studies were independently read by 2 blinded observers, by using a standardized scoring sheet. 4D-CTA results were analyzed with DSA as the criterion standard.

RESULTS: In 10 cases, there was full agreement between DSA and 4D-CTA regarding the Borden classification. However, in the remaining patient, a slow-filling DAVF with a low shunt volume was missed by both readers on 4D-CTA. In all 10 detected cases, ≥ 1 of the major contributing arteries could be identified with 4D-CTA. Although, by using DSA, the 2 observers identified additional arterial feeders in 7 and 8 cases, respectively, these discrepancies did not influence clinical decision making.

CONCLUSIONS: Although novel 4D-CTA imaging may not rule out a small slow-flow DAVF, it appears to be a valuable new adjunct in the noninvasive diagnostic work-up, treatment planning, and follow-up of patients with cranial DAVFs.

ABBREVIATIONS: CTA = CT angiography; DAVF = dural arteriovenous fistula; 4D-CTA = 4D (time-resolved) CTA; DSA = digital subtraction angiography; ECA = external carotid artery; ICA = internal carotid artery; IV = intravenous; MRA = MR angiography; trMRA = time-resolved MRA; VA = vertebral artery

DAVFs can either be asymptomatic or present with a variety of symptoms, including hemorrhage, focal neurologic deficits, chronic headache, bruit, dementia, seizures, or signs of intracranial hypertension.¹ The aggressiveness of a DAVF is related to its venous drainage pattern¹⁻⁴ (ie, whether its drainage is solely antegrade through a venous sinus or includes retrograde flow into cortical veins). Therefore, correct diagnosis and classification^{1,5} of a DAVF greatly influences the appropriate treatment strategy.

The criterion standard to demonstrate and classify the inappropriate filling of a pial vein or dural sinus from ≥ 1 dural artery, the hallmark of a DAVF, is conventional catheter-based angiography (DSA). Because DSA is relatively expensive and time-consuming and carries a rather high incidence of silent embolic events⁶ and a small risk of transient or permanent neurologic deterioration,⁷⁻⁹ a noninvasive alternative angiographic method is of interest. Moreover, patients with a DAVF may undergo multiple angiographic evaluations with time. In recent years, MRA and CTA have shown sufficient spatial resolution to answer many clinical neurovascular questions.¹⁰⁻¹² However, these vessel-cast techniques lack the temporal reso-

lution necessary to visualize arteriovenous shunts or venous drainage patterns.

More recently, time-resolved techniques have emerged for both MRA^{13,14} and CTA.¹⁵ Aside from generating cross-sectional images, these datasets enable visualization of blood-flow dynamics in cranial vessels with the first pass of an IV contrast bolus. Hence, it is conceivable that they may replace DSA in cases in which time-resolved imaging is required. We aimed to evaluate the capabilities and pitfalls of 4D-CTA in an initial series of patients who presented with a newly diagnosed DAVF, as demonstrated by DSA.

Materials and Methods

Patient Selection and Data Collection

Approval for this study was obtained from our institutional research ethics board in November 2008, and patients were admitted to the study between November 2008 and May 2009. Patients were included if DSA demonstrated a previously untreated DAVF. Exclusion criteria were patient age younger than 18 years, current treatment for diabetes mellitus, known allergy for iodinated contrast agents, renal failure (indicated by a baseline serum creatinine level of $>133 \mu\text{mol/L}$), inability to undergo 4D-CTA in <1 month from their DSA, and lack of informed consent.

After obtaining informed consent, we performed 4D-CTA imaging. Subsequently, all DSA and 4D-CTA studies were anonymized and independently evaluated by 1 radiologist and 1 neurosurgeon, by using a standardized scoring sheet (Table 1). The 4D-CTA results were scored first, and the DSA results were scored at least 24 hours later. Furthermore, we documented the mode of presentation and the

Received March 30, 2010; accepted after revision June 16.

From the Department of Radiology (P.W.A.W., P.A.B., K.G.t.), Leiden University Medical Center, Leiden, the Netherlands; and Department of Medical Imaging (J.J.B., K.G.t., T.K.), Toronto Western Hospital, Toronto, Ontario, Canada.

Please address correspondence to P.W.A. Willems, MD, PhD, Department of Radiology, Leiden University Medical Center, Postal Zone C2-S, PO Box 9600, 2300 RC Leiden, the Netherlands; e-mail: p.w.a.willems@lumc.nl

DOI 10.3174/ajnr.A2248

Table 1: Items scored by each reader for both DSA and 4D-CTA images

Item	Options
DAVF detected	Yes/no
Classification of Borden et al ⁵	
I	Drains through dural sinus
II	Retrograde flow from sinus into cortical veins
III	Direct flow into cortical veins
Classification of Cognard et al ¹	
I	Antegrade sinusoidal flow
II	Reflux: a) sinusoidal, b) arachnoid or both
III	Direct flow into cortical veins
IV	Same as III, but with venous ectasias
V	Flow into perimedullary veins
Arterial feeders, large	ECA ICA VA Any combination of the above
Arterial feeders, small	ECA: Occipital artery, auricular artery, superficial temporal artery, middle meningeal artery, ascending pharyngeal artery, internal maxillary artery ICA: Posterior group, inferolateral trunk, meningohypophyseal trunk, ophthalmic system VA: Muscular/occipital branches, posterior meningeal artery, posterior inferior cerebellar artery Any combination of the above
Fistula type	Single hole (focal)/multihole (diffuse)
Venous outflow obstruction	Yes/no
Isolated/trapped sinus	Yes/no

delay between the 2 studies as well as whether treatment was subsequently performed and, if so, whether involvement of the vessels used for treatment had been recognized in the 4D-CTA evaluation.

DSA Examination

Diagnostic intra-arterial DSA was performed with standard biplane fluoroscopy equipment (Infinix, Toshiba Medical Systems, Tochigi, Japan; or LCL-P, GE Healthcare, Buckinghamshire, United Kingdom). Because patients were only included in the study after DSA had demonstrated a DAVF, the angiographic protocol was not influenced by the study. It generally consisted of bilateral injections of the ICA, ECA, or VA, supplemented with selective injections of the occipital, ascending pharyngeal, or internal maxillary arteries, when indicated.

4D-CTA Examination

All 4D-CTA examinations were performed by using an Aquilion 1 multidetector CT scanner (Toshiba Medical Systems), equipped with 320 × 0.5 mm detector rows covering 16 cm of volume per rotation. Imaging was performed in the same manner as previously described.^{15,16} In short, a test-bolus acquisition at the level of the skull base was performed to optimize the timing of the dynamic acquisition sequence. Subsequently, IV infusion of 60 mL of nonionic contrast medium and 20 mL of saline was performed, followed by the dynamic acquisition sequence with a gantry rotation speed of 1 Hz. The dynamic acquisition sequence consisted of 1 mask volume (80 kVp, 300 mAs) and 22 dynamic volumes (80 kVp, 120 mAs). After subtracting the mask volume from the dynamic volumes, a total of 7040 (22 ×

Table 2: The frequencies of presenting symptoms according to the type of venous drainage, using the classification of Borden et al,⁵ as demonstrated with DSA

Borden Type	Presenting Symptoms		
	Incidental	Tinnitus	Hemorrhage
I	0	3	0
II	0	2	1
III	1	1	3

320) images were stored in DICOM files. The standard scanner software was capable of using these files to generate time-resolved (arterial-to-venous) volume renderings or maximum intensity projections by using any part of the cranial volume at any viewing angle. This study required at least anteroposterior and lateral maximum intensity projections from the entire cranial volume, reconstructed at 1-second intervals. Additional images could be used at the discretion of the reader.

Results

Between November 2008 and May 2009, 11 patients with a newly diagnosed DAVF were included, 8 men and 3 women. Their mean age was 52 ± 9.7 years. The mean delay between the 2 imaging modalities was 4 ± 4.0 days, with a maximum of 14 days. The frequencies of presenting symptoms according to Borden type⁵, as demonstrated by DSA, are shown in Table 2.

All DAVFs were detected by both readers on DSA. Ten of the 11 DAVFs were detected using 4D-CTA. The single case that remained undetected by 4D-CTA (Fig 1) was a slow-flow shunt with a low shunt volume and cortical venous drainage, which had presented with an intracranial hemorrhage. It was classified as a Borden grade III and Cognard¹ grade III lesion.

With regard to the 10 DAVFs that were detected in the 4D-CTA data, there was full agreement according to the Borden classification (see Fig 2 for an example). Both readers disagreed on the Cognard classification of 1 lesion, recording it as IIa+b on DSA and as IIb only on 4D-CTA data, recognizing the pial reflux but missing the retrograde sinusoidal flow (Fig 3).

Regarding feeding arteries, ≥1 of the major contributing arteries could be identified with 4D-CTA in all 10 detected cases. However, by using DSA, the 2 observers identified additional arterial feeders in 7 and 8 cases, respectively. When feeders were classified according to their territory (ECA, ICA, or VA), both readers showed discrepancies between DSA and 4D-CTA in 4 of 10 cases. In those cases, 4D-CTA results reflected the ECA supply to the DAVF correctly but failed to identify additional smaller feeders from the ICA and/or VA. When comparing separate branches from these territories, listed in Table 1 under “Arterial feeders, small,” 1 reader showed disagreement in 3 more cases and the other in 4 more cases. In such cases, only the largest feeders from a given territory were recognized in the 4D-CTA data (Fig 2).

With regard to the type of fistula (focal or diffuse) and the existence of venous obstruction or an isolated sinus, each reader individually showed full concordance between DSA and 4D-CTA. However, there was some disagreement between the 2 observers regarding these characteristics: In 4 cases, the readers disagreed as to whether the fistula was of a focal or diffuse nature; and in 2 cases, there was disagreement regarding the existence of venous outflow obstruction.

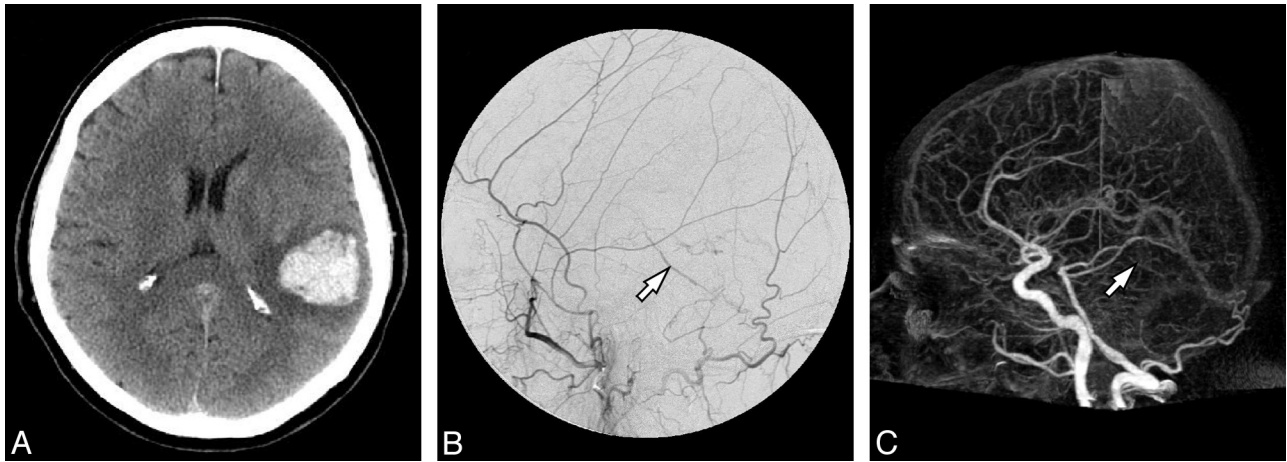


Fig 1. Imaging of a 65-year-old man who presented with an intracranial hemorrhage and whose DAVF was missed by 4D-CTA. *A*, Nonenhanced cranial CT scan on admission demonstrates the presenting hemorrhage. *B*, DSA, lateral view after left ECA injection, demonstrates abnormal retrograde filling of a pial vein (*arrow*), indicative of a DAVF. *C*, Lateral view of 4D-CTA, maximum intensity projection of the early venous phase, shows the same pial vein (*arrow*). Because visualization of the pial veins is expected on global opacification, only early filling would indicate a DAVF. However, due to the slow flow through the fistula, early venous filling could not be identified. Hence, this 4D-CTA study was read as having normal findings.

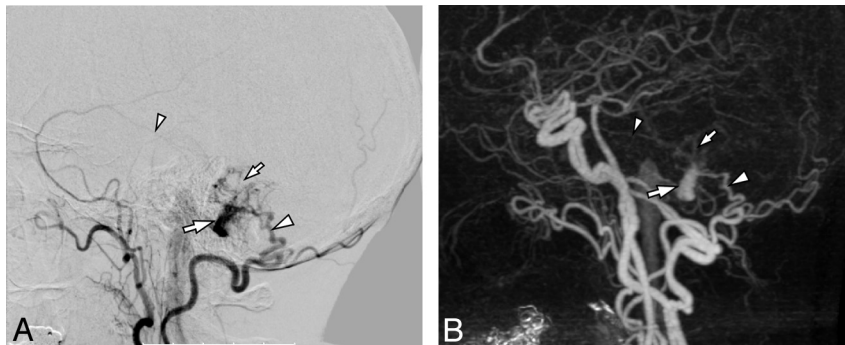


Fig 2. Imaging of a 60-year-old woman who presented with a right-sided pulse-synchronous tinnitus. *A*, DSA, lateral view after right ECA injection, demonstrates a DAVF (Borden I and Cognard I) at the level of the left sigmoid sinus (*large arrow*). The lesion is fed through a small arterial network (*small arrow*), which is mainly supplied by a branch from the occipital artery (*large arrowhead*) and to a lesser degree by a branch from the middle meningeal artery (*small arrowhead*). *B*, Lateral view of 4D-CTA, maximum intensity projection of late arterial phase, shows the early venous drainage into the right sigmoid sinus (*large arrow*). Compared with the DSA, the 4D-CTA is in agreement with regard to the site and classification of the lesion, as well as to its dominant feeder from the occipital artery (*large arrowhead*). However, although the smaller feeder from the middle meningeal artery can be seen (*small arrowhead*), neither reader had recorded it as such. The *small arrow* indicates the arterial network feeding the fistula.

Conservative management was chosen in 2 patients with a benign lesion who had presented with tinnitus. Endovascular treatment was attempted in the other 9 patients. A transvenous approach was chosen in 3 of these and a transarterial approach, in the remaining 6. In 4 of the 6 patients treated transarterially, 4D-CTA had correctly identified all feeding arteries used to gain access to the shunt to deposit embolic material.

The radiation dose involved in 4D-CTA imaging will vary, depending on the protocol used. With our current acquisition protocol, the total radiation dose received during 4D-CTA imaging amounted to 5.2 mSv. The radiation dose received during a DSA study is even more variable because it is dependent on many variables, such as the fluoroscopy time needed to navigate into vessels, the number of vessels studied, fluoroscopic parameters, type of fluoroscopic equipment, and so forth. In 4 typical DSA studies, the radiation dose was calculated to vary between 7.89 and 9.12 mSv. These calculations were based on Monte Carlo simulations by using the dose-area product values and beam geometry information. Ninety-five percent of this dose was estimated to have been delivered to the

cranium, with minor exposure of the thorax, abdomen, and pelvis.

Discussion

This study looked at the initial results of 4D-CTA in cranial DAVFs, compared with DSA, in an attempt to recognize the potential capabilities and pitfalls of 4D-CTA in such lesions.

In agreement with previous findings,³ all hemorrhages occurred in patients with a DAVF of Borden type II (1 patient) or III (1 patient). However, 1 DAVF incidentally found was of Borden type III and 3 of 5 patients with tinnitus as their only presenting symptom harbored a type II or III DAVF. Thus, mild or absent symptoms do not exclude the possibility of a potentially aggressive DAVF. These findings underline the necessity of an imaging tool capable not only of detecting the DAVF but also of describing its cortical venous reflux pattern, when present, because this is considered to be the major determining factor of the subsequent treatment strategy. The potential added advantage of 4D-CTA, aside from the fact that it is noninvasive and requires simple logistics, would be the availability of cross-sectional images. These could be helpful

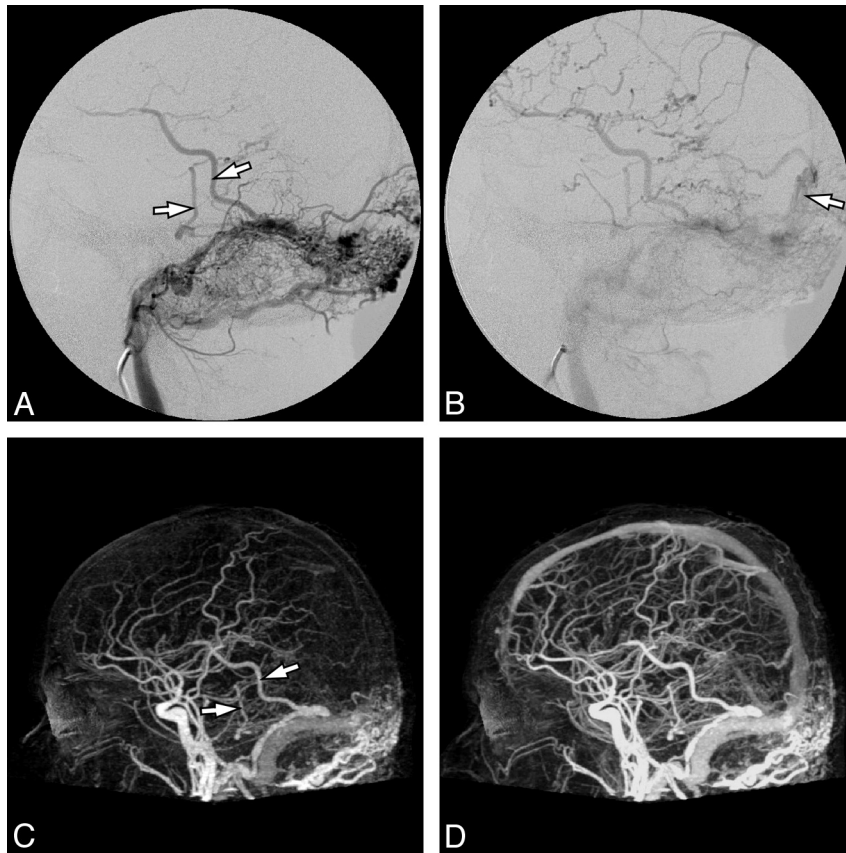


Fig 3. Imaging of a 47-year-old man who presented with a pulse-synchronous occipital bruit. *A*, DSA, lateral view after selective injection of the left occipital artery, demonstrates an extensive fistula at the torcular and left transverse sinus with cortical venous reflux (arrows). *B*, The later phase of the same injection demonstrates additional retrograde sinusoidal flow into the superior sagittal sinus (arrow). It was scored as Cognard grade IIa+b, due to both sinusoidal and pial reflux. *C*, Lateral view of 4D-CTA, maximum intensity projection of late arterial phase, shows early venous filling with cortical venous reflux (arrows). *D*, The venous phase of the same 4D-CTA study shows filling of the superior sagittal sinus, which is presumed to be antegrade. Because vascular opacification is nonselective, the temporal resolution is insufficient to recognize retrograde superior sagittal sinus filling. Thus, on the basis of this study, the lesion was erroneously scored as Cognard grade IIb.

for observing structural changes such as hydrocephalus or a hematoma or for surgical planning. Furthermore, perfusion maps may help determine whether the microcirculation of cerebral tissue is compromised by venous hypertension.¹⁷

An important finding of this study is the fact that 1 DAVF was not detected by 4D-CTA. Not only was the aggressiveness of this lesion demonstrated by its presentation with an intracranial hemorrhage, but the persisting cortical venous reflux also required urgent treatment. Not diagnosing this lesion correctly could have led to lack of treatment, exposing the patient to a high risk of future recurrent hemorrhage.^{4,18} This false-negative result was due to the fact that 4D-CTA opacification is nonselective and does not have the spatial and temporal resolution of DSA. In this patient, the fistula demonstrated slow flow, and venous filling was barely earlier than the “normal” venous phase. However, when selective ECA injections were performed, the opacification of cortical veins evidenced a DAVF.

When a DAVF was detected by 4D-CTA, our results clearly showed the spatial resolution to be insufficient to describe the angioarchitecture in detail. Although both readers were able to recognize the large feeding territories in 6 of 10 cases, accuracy dropped further when they were asked to describe feeding vessels in more detail. Even feeding arteries that proved useful during transarterial endovascular treatment were not recog-

nized in 2 of 6 cases. Again, these findings relate, at least in part, to the nonselectivity of the technique, rendering it difficult to judge whether arteries running close to the lesion do or do not connect to it. One may, however, argue that this type of angioarchitectural detail is not necessary to choose the appropriate treatment strategy and will become apparent in the diagnostic phase of an endovascular treatment session, if such treatment is elected.

Farb et al¹³ recently presented trMRA as a reliable tool in the diagnosis and classification of DAVFs in a “majority rule” setting with 3 readers. Because 4D-CTA is capable of generating datasets with both higher spatial and temporal resolution¹⁵ than trMRA, these results appear to contradict ours. We believe that this is due to the relatively small sample sizes in both studies. Farb et al expressed their concerns regarding small slow-flowing lesions, like the 1 missed by 4D-CTA in our series. Thus, caution is appropriate when one attempts to rule out a DAVF by using novel noninvasive angiographic techniques.

Nevertheless, our results show 4D-CTA to be a valuable new noninvasive tool in the diagnostic work-up and subsequent follow-up of patients with a cranial DAVF. Consequently, a larger prospective study is warranted to determine the diagnostic value of 4D-CTA in an unselected patient population. Until such results become available, we suggest per-

forming DSA when 4D-CTA findings are negative, before definitively ruling out a DAVF in a suspected patient.

Conclusions

We demonstrated the capabilities of 4D-CTA as a noninvasive dynamic imaging tool for the detection and grading of cranial DAVFs. Our results in 11 initial patients also demonstrated pitfalls of this novel technique, especially in slow-flow lesions. These are due to the nonselective nature of 4D-CTA and its lower spatial and temporal resolution compared with DSA. In conclusion, 4D-CTA appears to be a valuable new adjunct in the diagnostic work-up and subsequent follow-up of DAVFs, though it is not yet at the point of replacing DSA in all cases.

Acknowledgments

We thank Eric Salomon and Joost Roelofs, CT technologists, for their assistance with protocol, performance, and postprocessing of 4D-CTAs. We also thank Dirk Zweers, angiography technologist, for assisting with radiation dose calculations.

References

1. Cognard C, Gobin YP, Pierot L, et al. **Cerebral dural arteriovenous fistulas: clinical and angiographic correlation with a revised classification of venous drainage.** *Radiology* 1995;194:671–80
2. Lasjaunias P, Manelfe C, Chiu M. **Angiographic architecture of intracranial vascular malformations and fistulas: pretherapeutic aspects.** *Neurosurg Rev* 1986;9:253–63
3. Satomi J, van Dijk JM, terBrugge KG, et al. **Benign cranial dural arteriovenous fistulas: outcome of conservative management based on the natural history of the lesion.** *J Neurosurg* 2002;97:767–70
4. van Dijk JM, terBrugge KG, Willinsky RA, et al. **Clinical course of cranial dural arteriovenous fistulas with long-term persistent cortical venous reflux.** *Stroke* 2002;33:1233–36
5. Borden JA, Wu JK, Shucart WA. **A proposed classification for spinal and cranial dural arteriovenous fistulous malformations and implications for treatment.** *J Neurosurg* 1995;82:166–79
6. Bendszus M, Koltzenburg M, Burger R, et al. **Silent embolism in diagnostic cerebral angiography and neurointerventional procedures: a prospective study.** *Lancet* 1999;354:1594–97
7. Cloft HJ, Joseph GJ, Dion JE. **Risk of cerebral angiography in patients with subarachnoid hemorrhage, cerebral aneurysm, and arteriovenous malformation: a meta-analysis.** *Stroke* 1999;30:317–20
8. Kaufmann TJ, Huston J, Mandrekar JN, et al. **Complications of diagnostic cerebral angiography: evaluation of 19,826 consecutive patients.** *Radiology* 2007;243:812–19
9. Willinsky RA, Taylor SM, terBrugge K, et al. **Neurologic complications of cerebral angiography: prospective analysis of 2,899 procedures and review of the literature.** *Radiology* 2003;227:522–28
10. Agid R, Lee SK, Willinsky RA, et al. **Acute subarachnoid hemorrhage: using 64-slice multidetector CT angiography to “triage” patients’ treatment.** *Neuroradiology* 2006;48:787–94
11. Agid R, Willinsky RA, Lee SK, et al. **Characterization of aneurysm remnants after endovascular treatment: contrast-enhanced MR angiography versus catheter digital subtraction angiography.** *AJNR Am J Neuroradiol* 2008;29:1570–74
12. Uysal E, Oztora F, Ozel A, et al. **Detection and evaluation of intracranial aneurysms with 16-row multislice CT angiography: comparison with conventional angiography.** *Emerg Radiol* 2008;15:311–16
13. Farb RI, Agid R, Willinsky RA, et al. **Cranial dural arteriovenous fistula: diagnosis and classification with time-resolved MR angiography at 3T.** *AJNR Am J Neuroradiol* 2009;30:1546–51. Epub 2009 May 27
14. Krings T, Hans F. **New developments in MRA: time-resolved MRA.** *Neuroradiology* 2004;46(suppl 2):214–22
15. Brouwer PA, Bosman T, van Walderveen MA, et al. **Dynamic 320-section CT angiography in cranial arteriovenous shunting lesions.** *AJNR Am J Neuroradiol* 2010;31:767–70. Epub 2009 Oct 29
16. Salomon EJ, Barfett J, Willems PW, et al. **Dynamic CT angiography and CT perfusion employing a 320-detector row CT: protocol and current clinical applications.** *Klin Neuroradiol* 2009;19:187–96. Epub 2009 Aug 23
17. Klingebiel R, Siebert E, Diekmann S, et al. **4-D imaging in cerebrovascular disorders by using 320-slice CT: feasibility and preliminary clinical experience.** *Acad Radiol* 2009;16:123–29
18. Soderman M, Pavic L, Edner G, et al. **Natural history of dural arteriovenous shunts.** *Stroke* 2008;39:1735–39